

Received November 28, 2018, accepted December 25, 2018, date of publication January 31, 2019, date of current version January 22, 2020.

Digital Object Identifier 10.1109/ACCESS.2019.2895595

Real-Time Force Tracking Control of an Electro-Hydraulic System Using a Novel Robust Adaptive Sliding Mode Controller

LEI CHENG^{1,2}, ZHEN-CAI ZHU¹, GANG SHEN¹,
SHUJING WANG³, XIANG LI¹, AND YU TANG¹

¹Jiangsu Key Laboratory of Mine Mechanical and Electrical Equipment, School of Mechatronic Engineering, China University of Mining and Technology, Xuzhou 221116, China

²Xuzhou XCMG Environment Technology Company, Ltd., Xuzhou 221116, China

³The Army Engineering University Training Base of PLA, Xuzhou 221116, China

Corresponding author: Zhen-Cai Zhu (zhuzhencai@cumt.edu.cn)

This work was supported in part by the Key Project of National Natural Science Foundation of China under Grant U1510205, in part by the National Natural Science Foundation of China under Grant U1810124 and Grant 51805532, in part by the Program for Changjiang Scholars and Innovative Research Team in University under Grant IRT_16R68, and in part by the Priority Academic Program Development of Jiangsu Higher Education Institutions (PAPD).


ABSTRACT This article focuses on a novel robust adaptive sliding mode control strategy of an electro-hydraulic force loading system with consideration of external disturbances and parameter uncertainties. To obtain the proposed controller, the nonlinear dynamic model of the electro-hydraulic force loading system is firstly provided, where external disturbances and system's uncertain parameters are merged. Then, with consideration of external disturbances and parameter uncertainties, a robust adaptive sliding mode controller for the force control system is proposed and designed according to Lyapunov stability theory. The proposed controller has the merit of suppressing chattering phenomenon in traditional adaptive backstepping controllers when designing sign functions. In order to verify effectiveness and feasibility of the proposed controller, experimental studies are implemented on an electro-hydraulic force loading system by xPC rapid prototyping technology. Experimental results demonstrate that the proposed controller exhibits more excellent performance on force tracking control in comparison of a traditional proportional-integral controller and an adaptive backstepping controller.

INDEX TERMS Electro-hydraulic force loading system, adaptive backstepping controller, adaptive sliding mode controller, parameter uncertainties, external disturbances.

I. INTRODUCTION

Electro-hydraulic force loading systems (EHFLS) play an irreplaceable role in aerospace industry [1], automobile industry [2] and civil engineering [3], [4] for factitiously imitating the force loading imposed on a test specimen so as to evaluate original performance and potential problems of the specimen. EHFLS systems exhibit the superiorities of rapid response, large stiffness, and excellent force loading capability [5]–[8].

In the case of parameter uncertainties and external disturbances, the force tracking performance of EHFLS system has been extensively studied by scholars and various methods

The associate editor coordinating the review of this manuscript and approving it for publication was Chuxiong Hu .

have been proposed. The conventional Proportional-Integral-Derivative (PID) controller was applied by Alleyne in [9], from which it can be observed that traditional PID controller is insufficient for force tracking due to design limitations of the control parameters. In [10], Alleyne and Liu indicated that a satisfactory tracking performance cannot be ensured with a traditional PID controller for the EHFLS. To modify the deficiency of the traditional PID control method, a grey predictor fuzzy PID controller was proposed in [11] for a hybrid cylinder, which was employed to develop the force loading system. In [12], a force tracking control method of an aerodynamic load simulator was designed by the quantitative feedback theory (QFT). In order to realize real-time force tracking control of an electro-hydraulic road simulation system with external disturbances and parameter uncertainties,

a low-order QFT controller was presented in [13], and then a back-propagation control method was employed to online adjust QFT parameters in [14] so as to be suitable for a variety of work environments.

However, parameters uncertainties and external disturbances such as dynamics of hydraulic cylinder, dead zone, friction between cylinder rods and bores make high-accuracy control algorithms inaccessible for the EHFLS. Recently, various control algorithms for nonlinear systems have been proposed by scholars. The backstepping method is a systematic design approach based on Lyapunov function, which can ensure the closed-loop system's stability, tracking performance and transient characteristic for most strict-feedback systems [15]. Park [16] came up with a conventional backstepping control algorithm to guarantee the synchronization of a Genesio chaotic system. However, the above-mentioned control methods cannot account for parameters uncertainties. Therefore, the adaptive control strategy was utilized to address the system's uncertain parameters. A nonlinear adaptive controller with adaptive law is proposed in [17], [18] to deal with the nonlinear uncertain parameters caused by the change of the original control volume. In [19], taking the active motion disturbance, flow nonlinearities and parameter uncertainties into consideration, a high performance robust nonlinear adaptive controller was proposed for an electro-hydraulic force loading system. In order to overcome the issues resulted from the external disturbances, a novel robust adaptive excitation control method was designed in [20] for multimachine power systems. Guo *et al.* [21] presented a parameter adaptive backstepping controller to reject parameter uncertainties and unknown disturbance, which can improve the tracking performance of an electro-hydraulic system.

Owing to mature theories and numerous successful applications, sliding mode controller has been well-known in nonlinear control field. Ravandi *et al.* [22] combined fuzzy logic with traditional sliding mode controller for solving hybrid force and position control problem of a robot manipulator in uncertain environment. An adaptive sliding mode control algorithm is given in [23] for a class of nonlinear multiple-input multiple-output system subjected to external disturbances with consideration of system chattering. Plestan *et al.* [24] presented an adaptive version of sliding mode controller for displacement and force tracking control of a pneumatic actuator in view of parameter uncertainties and external disturbance. A hybrid force/position control method for a flexible joint robot based on the adaptive sliding mode control was proposed in [25].

In this work, the nonlinear model of the EHFLS in consideration of both external disturbances and parameter uncertainties is firstly established. Secondly, an adaptive backstepping controller considering external disturbances and parameter uncertainties is designed to improve force tracking performance in comparison of the common PID controller. Finally, in order to modify the imperfection caused by the sign function, a novel robust adaptive sliding mode

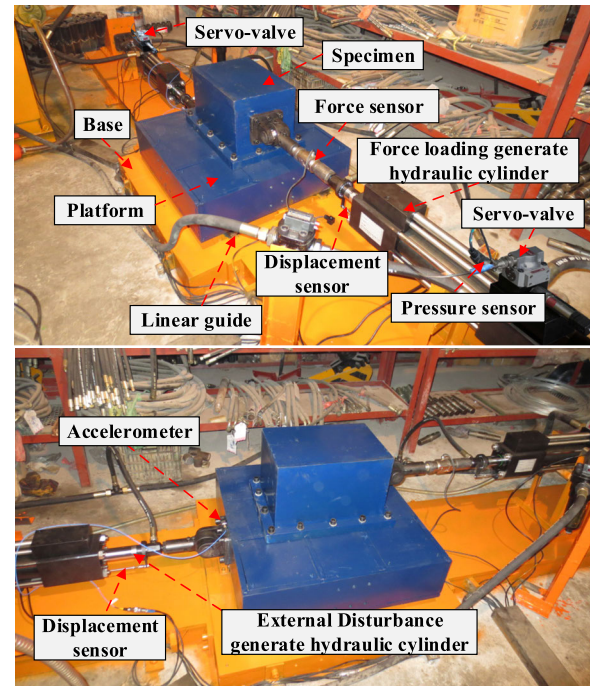


FIGURE 1. Experimental setup up for EHFLS.

controller (RASMC) is proposed to strengthen the system robustness.

The contents of this work are organized as follows. Dynamic model of the EHFLS and its experimental setup are shown in Section 2. The control methods utilized in this work are given in Section 3. Experimental validations on the EHFLS test bed are presented in Section 4. Concluding remarks are presented in Section 5.

II. EXPERIMENTAL SETUP AND SYSTEM MODELING

A. EXPERIMENTAL SETUP OF EHFLS

An experimental system of the EHFLS utilized to implement the proposed control strategies is presented in Figure 1. As shown in the figure, the experimental system consists of a real-time control system based on MATLAB/xPC target, a moving platform, a specimen, a force loading cylinder, an external disturbance cylinder, and a hydraulic power supply with 16Mpa supply pressure and 400 L/min flow capacity. The two hydraulic cylinders have 80 mm bore and 60 mm rod, and the cylinders are driven by two Moog servo-valves with 38 L/min flow capacity at 7MPa supply pressure. The two servo-valves are employed to exert loading force and generate external disturbance on the specimen, respectively. To obtain the real time force inflicted on the specimen, a force sensor is installed between the force loading hydraulic actuator and its corresponding spherical hinge. Two magnetostrictive displacement sensors are applied to measure real-time displacements of the force loading cylinder and the disturbance cylinder, respectively. The pressure difference of each hydraulic actuator's two chambers is obtained by two oil pressure sensors, respectively. A PCB accelerometer

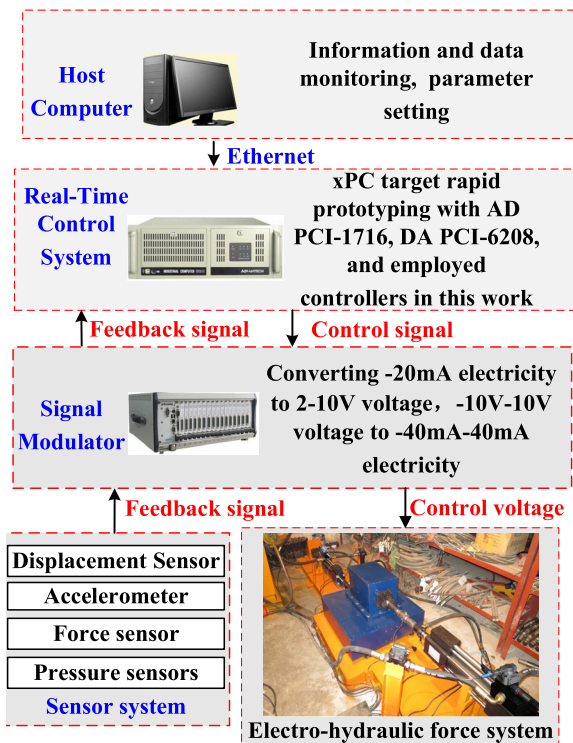


FIGURE 2. Control schematic diagram of EHFLS.

is mounted on the platform to measure the acceleration information.

Figure 2 demonstrates the physical implementation of control system for the discussed EHFLS, and the whole system is established based on xPC/target rapid prototyping technology. The control hardware is comprised of an Advantech IPC-610 computer, 16-bit A/D board PCI-1716 for collecting sensor signals, 16-bit D/A board PCI-6208 for sending out control signals, a host computer, and other auxiliary accessories. The Advantech computer is equipped with xPC/target real-time operating system, and both A/D and D/A boards are inserted in the PCI slots of the Advantech computer. The host computer provides a human-computer interaction interface for operators, and it is communicated with the Advantech computer by TCP/IP protocol. The proposed control algorithm together with other comparative methods is programmed on the host computer using MATLAB/Simulink, and then the real-time executable codes are generated by Microsoft Visual Studio. The sampling rate of the experimental system is chosen as 1000Hz so as to ensure an acceptable performance.

B. SYSTEM MODELING OF EHFLS

Figure 3 shows the working principle of electro-hydraulic cylinder that is used to generate force. The purpose of EHFLS is to make the hydraulic actuator track reference force as closely as possible. The nonlinear mathematical model of the EHFLS system is given as follows.

The first formulation to establish the system model of EHFLS is the force balance equation using the

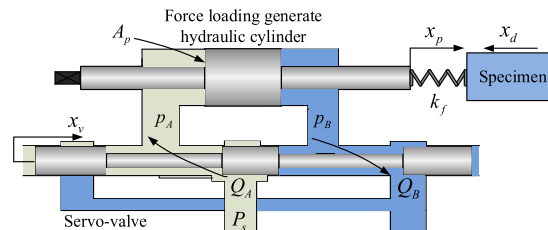


FIGURE 3. Actuating system for EHFLS.

Newton's second law, and it is given as follows

$$m_p \frac{d^2 x_p}{dt^2} = P_L A_p - B_p \frac{dx_p}{dt} - F_p \quad (1)$$

where x_p is displacement of the piston, m_p is equivalent mass acting on the piston for EHFLS, A_p is the effective acting area of the hydraulic actuator, P_L is pressure difference between two chambers of the actuator, B_p is external viscosity coefficient, and F_p is the imposed force for the tested specimen.

The second formulation for EHFLS modeling is the load flow continuity equation considering oil compressibility and leakage, and the load flow Q_L is described as

$$Q_L = A_p \frac{dx_p}{dt} + C_{ip} P_L + \frac{V_t}{4\beta_e} \frac{dP_L}{dt} \quad (2)$$

where C_{ip} is the total leakage coefficient expressed as $C_{ip} = C_{ip} + C_{ep}/2$, where C_{ip} and C_{ep} are internal and external leakage coefficient respectively, β_e is the oil effective bulk modulus, and V_t is the hydraulic actuator's total chamber volume.

In addition to the above two formulations, employing the Hooke's law principle, the force acting on the force sensor can be expressed as

$$F = k_f(x_p + x_d) \quad (3)$$

where k_f is the stiffness of force sensor, x_d is displacement of the disturbances generate hydraulic cylinder.

Referring to (1)-(3) and defining the system state variables $x = [x_1, x_2, x_3]^T = [F, \dot{x}_p, P_L]^T$, the nonlinear model of the discussed EHFLS can be transformed as

$$\begin{cases} \dot{x}_1 = k_f(x_2 + \dot{x}_d) + \Delta_1 \\ \dot{x}_2 = \theta_1 x_3 - \theta_2 x_2 - \theta_3 x_1 + \Delta_2 \\ \dot{x}_3 = -\theta_4 x_2 - \theta_5 x_3 + \theta_6 Q_L \end{cases} \quad (4)$$

where $\theta_1 = A_p/m_p$, $\theta_2 = B_p/m_p$, $\theta_3 = 1/m_p$, $\theta_4 = 4\beta_e A_p/V_t$, $\theta_5 = 4\beta_e C_{ip}/V_t$, $\theta_6 = 4\beta_e/V_t$, Δ_1 and Δ_2 are uncertain external disturbance, Q_L is regarded as the control input. As for system parameters of (4), the physical parameters B_p and C_{ip} are inevitably changing during experiment, which makes the force control of EHFLS more difficult.

III. CONTROLLER DESIGN

Figure 4 shows the framework of the proposed controller for the EHFLS, from which it can be seen that the proposed RSMC is composed of a sliding mode controller with adaptive laws. The proposed control method can modify

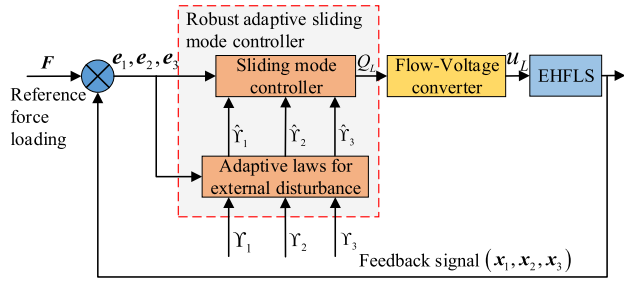


FIGURE 4. Block diagram of the RASMC.

traditional adaptive backstepping controllers by suppressing chattering phenomenon resulted from the design of sign function. The stability of the EHFLS with the proposed controller is guaranteed by Lyapunov stability theory. By means of the RASMC, the load flow from the valve to the chambers of the hydraulic actuator can be obtained, and then the practical output voltage to the servo valve can be obtained using a Flow-Voltage converter.

A. ADAPTIVE BACKSTEPPING CONTROLLER

Adaptive backstepping controller is an effective method for addressing the external disturbances and parameter uncertainties of a nonlinear system. In this article, the value of control input Q_L according to the adaptive backstepping control can be designed according to the following three steps.

Step 1: Define the force tracking error e_1 as

$$e_1 = x_1 - x_{1r} \tag{5}$$

where x_{1r} is the value of reference force.

Substituting (4) into (5), we obtain

$$\begin{aligned} \dot{e}_1 &= \dot{x}_1 - \dot{x}_{1r} \\ &= k_f x_2 + k_f \dot{x}_p + \Delta_1 - \dot{x}_{1r} \end{aligned} \tag{6}$$

Define the deviation of x_2 from its virtual control variable as

$$e_2 = x_2 - \alpha_1 \tag{7}$$

where α_1 is the virtual control variable of x_2 .

Construct a Lyapunov functional for (5) as

$$V_1 = \frac{1}{2} e_1^2 \tag{8}$$

and then the time derivative of V_1 with consideration of (7) can be expressed as follows

$$\begin{aligned} \dot{V}_1 &= e_1 \dot{e}_1 \\ &= e_1 (k_f e_2 + k_f \alpha_1 + k_f \dot{x}_p + \Delta_1 - \dot{x}_{1r}) \end{aligned} \tag{9}$$

Referring to (9), it can be seen that if $\alpha_1 = (-k_1 e_1 - k_f e_2 - k_f \dot{x}_p - \Delta_1 + \dot{x}_{1r}) / k_f$ and $k_1 \geq 0$, the time derivative of can be $\dot{V}_1 = -k_1 e_1^2 \leq 0$. However, since α_1 cannot contain e_2 and Δ_1 , so the virtual control should be designed as

$$\alpha_1 = \frac{1}{k_f} (-k_1 e_1 - k_f \dot{x}_p + \dot{x}_{1r}) \tag{10}$$

Substituting (10) into (9), the time derivative of V_1 is deduced as

$$\begin{aligned} \dot{V}_1 &= e_1 (-k_1 e_1 + k_f e_2 + \Delta_1) \\ &= -k_1 e_1^2 + k_f e_1 e_2 + \Delta_1 e_1 \end{aligned} \tag{11}$$

Remark 1: As can be observed in (11), the time derivative of V_1 is negative semi-definite if e_2 and Δ_1 are zero. Therefore, the next step is to make e_2 and Δ_1 equal to zero.

Step 2: Referring to (10), we have

$$\begin{aligned} \dot{\alpha}_1 &= \frac{1}{k_f} (-k_1 \dot{e}_1 - k_f \ddot{x}_p + \ddot{x}_{1r}) \\ &= \frac{1}{k_f} (-k_1 (k_f x_2 + k_f \dot{x}_p + \Delta_1 - \dot{x}_{1r}) - k_f \ddot{x}_p + \ddot{x}_{1r}) \end{aligned} \tag{12}$$

and then substituting (4) and (12) into (7), we obtain

$$\begin{aligned} \dot{e}_2 &= \dot{x}_2 - \dot{\alpha}_1 \\ &= \theta_1 x_3 - \theta_2 x_2 - \theta_3 x_1 + \Delta_2 - \dot{\alpha}_1 \end{aligned} \tag{13}$$

Defining the parametric error as $\tilde{\theta}_2 = \hat{\theta}_2 - \theta_2$, where $\hat{\theta}_2$ is the estimated value and θ_2 is the actual unknown, the time derivative of e_2 can be rewritten as

$$\dot{e}_2 = \theta_1 x_3 - (\hat{\theta}_2 - \tilde{\theta}_2) x_2 - \theta_3 x_1 + \Delta_2 - \dot{\alpha}_1 \tag{14}$$

Next, defining Lyapunov function V_2 as

$$V_2 = V_1 + \frac{1}{2} e_2^2 + \frac{1}{2\gamma_2} \tilde{\theta}_2^2 \tag{15}$$

where γ_2 is the gain of parameter update law for $\hat{\theta}_2$. It is reasonable to assume that the unknown parameter θ_2 is slowly changed, and then time derivative of V_2 can be written as

$$\begin{aligned} \dot{V}_2 &= \dot{V}_1 + e_2 \dot{e}_2 + \frac{1}{\gamma_2} \tilde{\theta}_2 \dot{\tilde{\theta}}_2 \\ &= -k_1 e_1^2 + \Delta_1 e_1 + e_2 [k_f e_1 + \theta_1 x_3 - \hat{\theta}_2 x_2 - \theta_3 x_1 \\ &\quad - \frac{1}{k_f} (-k_1 k_f x_2 - k_1 k_f \dot{x}_p + k_1 \dot{x}_{1r} - k_f \ddot{x}_p + \ddot{x}_{1r})] \\ &\quad + e_2 \tilde{\theta}_2 x_2 + e_2 \Delta_2 + \frac{e_2 k_1}{k_f} \Delta_1 + \frac{1}{\gamma_2} \tilde{\theta}_2 \dot{\tilde{\theta}}_2 \end{aligned} \tag{16}$$

Defining the virtual control variable of x_3 as α_2 , the deference between x_3 and α_2 can be expressed as

$$e_3 = x_3 - \alpha_2 \tag{17}$$

Substituting (17) into (7) yields that

$$\begin{aligned} \alpha_2 &= \frac{1}{\theta_1} (-k_2 e_2 - k_f e_1 + \hat{\theta}_2 x_2 + \theta_3 x_1 - k_1 x_2 \\ &\quad - k_1 \dot{x}_p + \frac{k_1}{k_f} \dot{x}_{1r} - \ddot{x}_p + \frac{1}{k_f} \ddot{x}_{1r}) \end{aligned} \tag{18}$$

where $k_2 \geq 0$.

Substituting (18) into (16), time derivative of V_2 can be deduced as

$$\begin{aligned} \dot{V}_2 &= -k_1 e_1^2 - k_2 e_2^2 + \theta_1 e_2 e_3 + e_2 \Delta_2 \\ &\quad + (e_1 + \frac{e_2 k_1}{k_f}) \Delta_1 + \tilde{\theta}_2 \gamma_2^{-1} (\dot{\tilde{\theta}}_2 + \gamma_2 e_2 x_2) \end{aligned} \tag{19}$$

Remark 2: As can be seen, (19) is negative semi-definite provided that e_3 and Δ_2 are zero. Therefore, the next step is to make e_3 and Δ_2 equal to zero.

Step 3: As the final controlled variable x_2 is visualized, virtual control variable is no longer needed at this step.

Referring to (18), time derivative of α_2 can be expressed as

$$\begin{aligned} \dot{\alpha}_2 &= \frac{1}{\theta_1}(-k_2\dot{e}_2 - k_f\dot{e}_1 + \hat{\theta}_2x_2 + \hat{\theta}_2\dot{x}_2 + \theta_3\dot{x}_1 \\ &\quad - k_1\dot{x}_2 - k_1\ddot{x}_{fe} + \frac{k_1}{k_f}\ddot{x}_{1r} - \ddot{x}_p + \frac{1}{k_f}\ddot{x}_{1r}) \\ &= A\theta_2 + B\theta_3 + C + D\Delta_1 + E\Delta_2 \end{aligned} \quad (20)$$

where

$$\begin{aligned} A &= \frac{k_2x_2 - \hat{\theta}_2x_2 + k_1x_2}{\theta_1} \\ B &= \frac{k_2x_1 - \hat{\theta}_2x_1 + k_1x_1 + k_f(x_2 + \dot{x}_p)}{\theta_1} \\ C &= -k_2x_3 + \hat{\theta}_2x_3 - k_1x_3 \\ &\quad + \frac{-k_1k_2x_2 + k_1k_2\dot{x}_d + \frac{k_1k_2}{k_f}\dot{x}_{1r} + k_2k_f\ddot{x}_p - k_2\ddot{x}_{1r} - k_f^2x_2}{\theta_1} \\ &\quad + \frac{-k_f^2\dot{x}_p + k_f\dot{x}_{1r} + \hat{\theta}_2x_2 - k_1\ddot{x}_p + \frac{k_1}{k_f}\ddot{x}_{1r} - \ddot{x}_p + \frac{\ddot{x}_{1r}}{k_f}}{\theta_1} \end{aligned}$$

$$D = -\frac{k_1k_2}{k_f} - k_f + \theta_3$$

$$E = -k_2 + \hat{\theta}_2 - k_1$$

Combining the (21) and (24), we obtain

$$\begin{aligned} \dot{e}_3 &= \dot{x}_3 - \dot{\alpha}_2 \\ &= -\theta_4x_2 - \theta_5x_3 - \theta_6Q_L - A\theta_2 \\ &\quad - B\theta_3 - C - D\Delta_1 - E\Delta_2 \end{aligned} \quad (21)$$

To deal with the unknown parameters θ_4 and θ_5 , the estimated values $\hat{\theta}_4$ and $\hat{\theta}_5$ are defined. The differences between the estimated value and the unknown parameter is expressed as $\tilde{\theta}_4 = \hat{\theta}_4 - \theta_4$, $\tilde{\theta}_5 = \hat{\theta}_5 - \theta_5$, and then (21) can be rewritten as

$$\begin{aligned} \dot{e}_3 &= -(\hat{\theta}_4 - \tilde{\theta}_4)x_2 - (\hat{\theta}_5 - \tilde{\theta}_5)x_3 - \theta_6Q_L \\ &\quad - A(\hat{\theta}_2 - \tilde{\theta}_2) - B\theta_3 - C - D\Delta_1 - E\Delta_2 \end{aligned} \quad (22)$$

Defining Lyapunov function

$$V_3 = V_2 + \frac{1}{2}e_3^2 + \frac{1}{2\gamma_4}\tilde{\theta}_4^2 + \frac{1}{2\gamma_5}\tilde{\theta}_5^2 \quad (23)$$

where γ_4 and γ_5 are parameter updating gains for $\hat{\theta}_4$ and $\hat{\theta}_5$, respectively. Similarly, the unknown parameters θ_4 , θ_5 are also regarded as slowly changed, and we can obtain

$$\begin{aligned} \dot{V}_3 &= \dot{V}_2 + e_3\dot{e}_3 + \frac{1}{\gamma_4}\tilde{\theta}_4\dot{\hat{\theta}}_4 + \frac{1}{\gamma_5}\tilde{\theta}_5\dot{\hat{\theta}}_5 \\ &= -k_1e_1^2 - k_2e_2^2 + e_3[\theta_1e_2 - (\hat{\theta}_4 - \tilde{\theta}_4)x_2 - (\hat{\theta}_5 - \tilde{\theta}_5)x_3 + \theta_6Q_L \\ &\quad - A(\hat{\theta}_2 - \tilde{\theta}_2) - B\theta_3 - C - D\Delta_1 - E\Delta_2] + e_2\Delta_2 \end{aligned}$$

$$\begin{aligned} &+ (e_1 + \frac{e_2k_1}{k_f})\Delta_1 + \tilde{\theta}_2r_2^{-1}(\dot{\hat{\theta}}_2 + \gamma_2e_2x_2) + \frac{1}{\gamma_4}\tilde{\theta}_4\dot{\hat{\theta}}_4 + \frac{1}{\gamma_5}\tilde{\theta}_5\dot{\hat{\theta}}_5 \\ &= -k_1e_1^2 - k_2e_2^2 + e_3(\theta_1e_2 - \hat{\theta}_4x_2 - \hat{\theta}_5x_3 + \theta_6Q_L - A\hat{\theta}_2 - B\theta_3 \\ &\quad - C - D\Delta_1 - E\Delta_2) + \Delta_1e_1 + (\Delta_2 + \frac{\Delta_1k_1}{k_f})e_2 + \tilde{\theta}_2\gamma_2^{-1}(\dot{\hat{\theta}}_2 \\ &\quad + \gamma_2(e_2x_2 + Ae_3)) + \tilde{\theta}_4r_4^{-1}(\dot{\hat{\theta}}_4 + \gamma_4e_3x_2) \\ &\quad + \tilde{\theta}_5\gamma_5^{-1}(\dot{\hat{\theta}}_5 + \gamma_5e_3x_3) \end{aligned} \quad (24)$$

Next, the actual controlled variable Q_L can be designed as

$$\begin{aligned} Q_L &= \frac{1}{\theta_6}[-k_3e_3 - \theta_1e_2 + \hat{\theta}_4x_2 + \hat{\theta}_5x_3 + A\hat{\theta}_2 + B\theta_3 \\ &\quad + C + F_3\text{sgn}(e_3)] - \frac{e_1}{e_3}F_1\text{sgn}(e_1) - \frac{e_2}{e_3}F_2\text{sgn}(e_2) \end{aligned} \quad (25)$$

where $F_1 \geq |\Delta_1|$, $F_2 \geq \left| \Delta_2 + \frac{\Delta_1k_1}{k_f} \right|$, $F_3 \geq |D\Delta_1 + E\Delta_2|$, and sgn is defined as

$$\text{sgn}(\alpha) = \begin{cases} 1 & \text{if } \alpha > 0 \\ 0 & \text{if } \alpha = 0 \\ -1 & \text{if } \alpha < 0 \end{cases} \quad (26)$$

Combing (24) and (25), the time derivative of V_3 can be rewritten as

$$\begin{aligned} \dot{V}_3 &= -k_1e_1^2 - k_2e_2^2 - k_3e_3^2 + e_1[\Delta_1 - F_1\text{sgn}(e_1)] \\ &\quad + e_2[\Delta_2 + \frac{\Delta_1k_1}{k_f} - F_2\text{sgn}(e_2)] + e_3[-(D\Delta_1 + E\Delta_2) \\ &\quad - F_3\text{sgn}(e_3)] + \tilde{\theta}_2\gamma_2^{-1}(\dot{\hat{\theta}}_2 + \gamma_2(e_2x_2 + Ae_3)) \\ &\quad + \tilde{\theta}_4\gamma_4^{-1}(\dot{\hat{\theta}}_4 + \gamma_4e_3x_2) + \tilde{\theta}_5\gamma_5^{-1}(\dot{\hat{\theta}}_5 + \gamma_5e_3x_3) \end{aligned} \quad (27)$$

To guarantee the stability of EHFLS, the value of $\dot{\hat{\theta}}_2$, $\dot{\hat{\theta}}_4$ and $\dot{\hat{\theta}}_5$ are chosen as follows

$$\dot{\hat{\theta}}_2 = -\gamma_2(e_2x_2 + Ae_3) \quad (28)$$

$$\dot{\hat{\theta}}_4 = -\gamma_4e_3x_2 \quad (29)$$

$$\dot{\hat{\theta}}_5 = -\gamma_5e_3x_3 \quad (30)$$

and then we can obtain

$$\begin{aligned} \dot{V}_3 &= -k_1e_1^2 - k_2e_2^2 - k_3e_3^2 + e_1[\Delta_1 - F_1\text{sgn}(e_1)] \\ &\quad + e_2[\Delta_2 + \frac{\Delta_1k_1}{k_f} - F_2\text{sgn}(e_2)] + e_3[-(D\Delta_1 + E\Delta_2) \\ &\quad - F_3\text{sgn}(e_3)] \leq 0 \end{aligned} \quad (31)$$

B. ROBUST ADAPTIVE SLIDING MODE CONTROLLER

Referring to (25), it is obvious that the actual controlled variable Q_L contain three sign signal items. Moreover, the signal items are related to three different errors, which increases the difficulty of parameters design. In addition, the gains of parameters update law for $\hat{\theta}_2$, $\hat{\theta}_4$, and $\hat{\theta}_5$ also needs to be selected. To address the above-mentioned issues, the following state space function that combines the parameter

uncertainties and external disturbances is given as

$$\begin{cases} \dot{x}_1 = k_f(x_2 + \dot{x}_d) + \Upsilon_1 \\ \dot{x}_2 = \theta_1 x_3 - \hat{\theta}_2 x_2 - \hat{\theta}_3 x_1 + \Upsilon_2 \\ \dot{x}_3 = -\hat{\theta}_4 x_2 - \hat{\theta}_5 x_3 + \theta_6 Q_L + \Upsilon_3 \end{cases} \quad (32)$$

As for the modified state space function, the proposed robust adaptive sliding mode controller is designed according to the following steps.

Step 1: Similar with the design process of the adaptive backstepping controller, defining force tracking error \bar{e}_1 as

$$\bar{e}_1 = x_1 - x_{1r} \quad (33)$$

Defining a virtual control variable as

$$\bar{\alpha}_1 = c_1 \bar{e}_1 \quad (34)$$

and then combining force tracking error \bar{e}_1 and virtual control variable $\bar{\alpha}_1$, another error is expressed as

$$\bar{e}_2 = \dot{\bar{e}}_1 + \bar{\alpha}_1 = \dot{\bar{e}}_1 + c_1 \bar{e}_1 \quad (35)$$

Defining Lyapunov function

$$\bar{V}_1 = \frac{1}{2} \bar{e}_1^2 \quad (36)$$

Combing (33) and (35), we obtain

$$\begin{aligned} \dot{\bar{V}}_1 &= \bar{e}_1 \dot{\bar{e}}_1 = \bar{e}_1(\dot{\bar{e}}_2 - c_1 \bar{e}_1) \\ &= -c_1 \bar{e}_1^2 + \bar{e}_1 \bar{e}_2 \end{aligned} \quad (37)$$

Step 2: Defining a virtual control variable as

$$\bar{\alpha}_2 = c_2 \bar{e}_2 \quad (38)$$

and combining error \bar{e}_2 and virtual control variable $\bar{\alpha}_2$, another error is expressed as

$$\bar{e}_3 = \dot{\bar{e}}_2 + \bar{\alpha}_2 = \dot{\bar{e}}_2 + c_2 \bar{e}_2 \quad (39)$$

Constructing a Lyapunov functional for error \bar{e}_2 as

$$\bar{V}_2 = \bar{V}_1 + \frac{1}{2} \bar{e}_2^2 \quad (40)$$

and then we obtain

$$\begin{aligned} \dot{\bar{V}}_2 &= \dot{\bar{V}}_1 + \bar{e}_2 \dot{\bar{e}}_2 \\ &= -c_1 \bar{e}_1^2 + \bar{e}_1 \bar{e}_2 + \bar{e}_2(\dot{\bar{e}}_3 - c_2 \bar{e}_2) \\ &= -c_1 \bar{e}_1^2 + \bar{e}_1 \bar{e}_2 - c_2 \bar{e}_2^2 + \bar{e}_2 \bar{e}_3 \end{aligned} \quad (41)$$

According to (40), the time derivative of \bar{e}_3 can be deduced as

$$\begin{aligned} \dot{\bar{e}}_3 &= \ddot{\bar{e}}_2 + \dot{\bar{\alpha}}_2 = \ddot{\bar{e}}_2 + c_2 \dot{\bar{e}}_2 \\ &= \ddot{\bar{e}}_1 + c_1 \dot{\bar{e}}_1 + c_2 \dot{\bar{e}}_2 \\ &= \ddot{x}_1 - \ddot{x}_{1r} + c_1(\dot{x}_1 - \dot{x}_{1r}) + c_2(\ddot{e}_1 + c_1 \dot{e}_1) \\ &= \ddot{x}_1 - \ddot{x}_{1r} + c_1(\dot{x}_1 - \dot{x}_{1r}) + c_2(\dot{x}_1 - \dot{x}_{1r}) + c_1 c_2(\dot{x}_1 - \dot{x}_{1r}) \end{aligned} \quad (42)$$

Step 3: Defining a sliding mode switching function

$$\sigma = \bar{k}_1 \bar{e}_1 + \bar{k}_2 \bar{e}_2 + \bar{e}_3 \quad (43)$$

and defining a Lyapunov function for the sliding mode switching function σ as

$$\bar{V}_3 = \bar{V}_2 + \frac{1}{2} \sigma^2 \quad (44)$$

the following result can be concluded

$$\begin{aligned} \dot{\bar{V}}_3 &= \dot{\bar{V}}_2 + \sigma \dot{\sigma} \\ &= -c_1 \bar{e}_1^2 + \bar{e}_1 \bar{e}_2 - c_2 \bar{e}_2^2 + \bar{e}_2 \bar{e}_3 + \sigma \dot{\sigma} \\ &= -c_1 \bar{e}_1^2 + \bar{e}_1 \bar{e}_2 - c_2 \bar{e}_2^2 + \bar{e}_2 \bar{e}_3 + \sigma(\bar{k}_1 \dot{\bar{e}}_1 + \bar{k}_2 \dot{\bar{e}}_2 + \dot{\bar{e}}_3) \\ &= -c_1 \bar{e}_1^2 + \bar{e}_1 \bar{e}_2 - c_2 \bar{e}_2^2 + \bar{e}_2 \bar{e}_3 + \sigma[\bar{k}_1(\dot{\bar{e}}_2 - c_1 \bar{e}_1) \\ &\quad + \bar{k}_2(\dot{\bar{e}}_3 - c_2 \bar{e}_2) + \dot{\bar{e}}_3] \\ &= -c_1 \bar{e}_1^2 + \bar{e}_1 \bar{e}_2 - c_2 \bar{e}_2^2 + \bar{e}_2 \bar{e}_3 \\ &\quad + \sigma[\bar{k}_1(\dot{\bar{e}}_2 - c_1 \bar{e}_1) + \bar{k}_2(\dot{\bar{e}}_3 - c_2 \bar{e}_2) \\ &\quad + \ddot{x}_1 - \ddot{x}_{1r} + c_1(\dot{x}_1 - \dot{x}_{1r}) + c_2(\dot{x}_1 - \dot{x}_{1r}) \\ &\quad + c_1 c_2(\dot{x}_1 - \dot{x}_{1r})] \\ &= -c_1 \bar{e}_1^2 + \bar{e}_1 \bar{e}_2 - c_2 \bar{e}_2^2 + \bar{e}_2 \bar{e}_3 + \sigma[\bar{k}_1(\dot{\bar{e}}_2 - c_1 \bar{e}_1) \\ &\quad + \bar{k}_2(\dot{\bar{e}}_3 - c_2 \bar{e}_2) \\ &\quad + f(\ddot{x}_1, \ddot{x}_{1r}, \dot{x}_1, \dot{x}_{1r}, \dot{x}_1, \dot{x}_{1r}) + \kappa_0 Q_L \\ &\quad + \kappa_1 \Upsilon_1 + \kappa_2 \Upsilon_2 + \kappa_3 \Upsilon_3] \end{aligned} \quad (45)$$

where $\kappa_0, \kappa_1, \kappa_2,$ and κ_3 are the combine like terms in (45).

Referring to (45), we obtain

$$\begin{aligned} Q_L &= (-\bar{k}_1(\dot{\bar{e}}_2 - c_1 \bar{e}_1) - \bar{k}_2(\dot{\bar{e}}_3 - c_2 \bar{e}_2) - h(\sigma + \beta \text{sgn}(\sigma)) \\ &\quad - f(\ddot{x}_1, \ddot{x}_{1r}, \dot{x}_1, \dot{x}_{1r}, \dot{x}_1, \dot{x}_{1r}) - \bar{\Upsilon}_1 \text{sgn}(\sigma) \\ &\quad - \bar{\Upsilon}_2 \text{sgn}(\sigma) - \bar{\Upsilon}_3 \text{sgn}(\sigma))/\kappa_0 \end{aligned} \quad (46)$$

where $\bar{\Upsilon}_1 \geq |\kappa_1 \Upsilon_1|, \bar{\Upsilon}_2 \geq |\kappa_2 \Upsilon_2|,$ and $\bar{\Upsilon}_3 \geq |\kappa_3 \Upsilon_3|.$

Next, combining (45) and (46), we obtain

$$\begin{aligned} \dot{\bar{V}}_3 &= -c_1 \bar{e}_1^2 + \bar{e}_1 \bar{e}_2 - c_2 \bar{e}_2^2 + \bar{e}_2 \bar{e}_3 - h\sigma^2 - h\beta |\sigma| \\ &\quad + \kappa_1 \Upsilon_1 - \bar{\Upsilon}_1 \text{sgn}(\sigma) + \kappa_2 \Upsilon_2 - \bar{\Upsilon}_2 \text{sgn}(\sigma) \\ &\quad + \kappa_3 \Upsilon_3 - \bar{\Upsilon}_3 \text{sgn}(\sigma) \\ &\leq -c_1 \bar{e}_1^2 + \bar{e}_1 \bar{e}_2 - c_2 \bar{e}_2^2 + \bar{e}_2 \bar{e}_3 - h\sigma^2 - h\beta |\sigma| \end{aligned} \quad (47)$$

where h and β are designed positive constant.

According to (43), the following result is concluded

$$\begin{aligned} h\sigma^2 &= h(\bar{k}_1^2 \bar{e}_1^2 + 2\bar{k}_1 \bar{k}_2 \bar{e}_1 \bar{e}_2 + 2\bar{k}_1 \bar{e}_1 \bar{e}_3 \\ &\quad + 2\bar{k}_2 \bar{e}_2 \bar{e}_3 + \bar{k}_2^2 \bar{e}_2^2 + \bar{e}_3^2) \end{aligned} \quad (48)$$

Defining a matrix as follows

$$Q = \begin{bmatrix} h\bar{k}_1^2 + c_1 & h\bar{k}_1 \bar{k}_2 - \frac{1}{2} & h\bar{k}_1 \\ h\bar{k}_1 \bar{k}_2 - \frac{1}{2} & h\bar{k}_2^2 + c_2 & h\bar{k}_2 - \frac{1}{2} \\ h\bar{k}_1 & h\bar{k}_2 - \frac{1}{2} & h \end{bmatrix} \quad (49)$$

and then we obtain

$$\begin{aligned}
 & e^T Q e \\
 &= [\bar{e}_1 \quad \bar{e}_2 \quad \bar{e}_3] \begin{bmatrix} h\bar{k}_1^2 + c_1 & h\bar{k}_1 k_2 - \frac{1}{2} & h\bar{k}_1 \\ h\bar{k}_1 \bar{k}_2 - \frac{1}{2} & h\bar{k}_2^2 + c_2 & h\bar{k}_2 - \frac{1}{2} \\ h\bar{k}_1 & h\bar{k}_2 - \frac{1}{2} & h \end{bmatrix} \\
 & [\bar{e}_1 \quad \bar{e}_2 \quad \bar{e}_3]^T \\
 &= h\bar{k}_1^2 \bar{e}_1^2 + 2h\bar{k}_1 \bar{k}_2 \bar{e}_1 \bar{e}_2 + 2h\bar{k}_1 \bar{e}_1 \bar{e}_3 + 2h\bar{k}_2 \bar{e}_2 \bar{e}_3 \\
 & \quad + h\bar{k}_2^2 \bar{e}_2^2 + h\bar{e}_3^2 - c_1 \bar{e}_1^2 + \bar{e}_1 \bar{e}_2 - c_2 \bar{e}_2^2 + \bar{e}_2 \bar{e}_3 \quad (50)
 \end{aligned}$$

where $e = [\bar{e}_1 \quad \bar{e}_2 \quad \bar{e}_3]$.

If the matrix Q can be positive definite, we obtain

$$\dot{\bar{V}}_3 \leq -e^T Q e - h\beta |\sigma| \leq 0 \quad (51)$$

Since

$$|Q| = \frac{1}{2} h k_1 - \frac{1}{4} h - \frac{1}{4} c_1 - \frac{1}{2} h k_1^2 + c_1 c_2 h + c_1 h k_2 \quad (52)$$

By selecting appropriate values of h , c_1 , c_2 , \bar{k}_1 , and \bar{k}_2 , the matrix Q can be positive definite. Then, we obtain $\dot{\bar{V}}_3 \leq 0$, which ensure the stability of system.

As can be seen from the (46), there are also four sign function need to be designed, which may result in chattering phenomenon on the system. To further improve the control input, define estimate values of the combination values of external disturbances and parameter uncertainties as $\hat{\Upsilon}_1$, $\hat{\Upsilon}_2$, and $\hat{\Upsilon}_3$. Then, the parameters' estimation error can be defined as $\tilde{\Upsilon}_1$, $\tilde{\Upsilon}_2$, and $\tilde{\Upsilon}_3$, where $\tilde{\Upsilon}_1 = \hat{\Upsilon}_1 - \Upsilon_1$, $\tilde{\Upsilon}_2 = \hat{\Upsilon}_2 - \Upsilon_2$, and $\tilde{\Upsilon}_3 = \hat{\Upsilon}_3 - \Upsilon_3$.

Defining Lyapunov function

$$\bar{V}_4 = \bar{V}_3 + \frac{1}{2\varepsilon_1} \tilde{\Upsilon}_1^2 + \frac{1}{2\varepsilon_2} \tilde{\Upsilon}_2^2 + \frac{1}{2\varepsilon_3} \tilde{\Upsilon}_3^2 \quad (53)$$

and then we obtain

$$\begin{aligned}
 \dot{\bar{V}}_4 &= \dot{\bar{V}}_3 + \frac{1}{\varepsilon_1} \tilde{\Upsilon}_1 \dot{\hat{\Upsilon}}_1 + \frac{1}{\varepsilon_2} \tilde{\Upsilon}_2 \dot{\hat{\Upsilon}}_2 + \frac{1}{\varepsilon_3} \tilde{\Upsilon}_3 \dot{\hat{\Upsilon}}_3 \\
 &= -c_1 \bar{e}_1^2 + \bar{e}_1 \bar{e}_2 - c_2 \bar{e}_2^2 + \bar{e}_2 \bar{e}_3 + \sigma [\bar{k}_1 (\bar{e}_2 - c_1 \bar{e}_1) \\
 & \quad + \bar{k}_2 (\bar{e}_3 - c_2 \bar{e}_2) \\
 & \quad + f(\ddot{x}_1, \ddot{x}_{1r}, \dot{x}_1, \dot{x}_{1r}, \dot{x}_1, \dot{x}_{1r}) + \kappa_0 Q_L + \kappa_1 \Upsilon_1 \\
 & \quad + \kappa_2 \Upsilon_2 + \kappa_3 \Upsilon_3] \\
 & \quad + \frac{1}{\varepsilon_1} \tilde{\Upsilon}_1 \dot{\hat{\Upsilon}}_1 + \frac{1}{\varepsilon_2} \tilde{\Upsilon}_2 \dot{\hat{\Upsilon}}_2 + \frac{1}{\varepsilon_3} \tilde{\Upsilon}_3 \dot{\hat{\Upsilon}}_3 \\
 &= -c_1 \bar{e}_1^2 + \bar{e}_1 \bar{e}_2 - c_2 \bar{e}_2^2 + \bar{e}_2 \bar{e}_3 + \sigma [\bar{k}_1 (\bar{e}_2 - c_1 \bar{e}_1) \\
 & \quad + \bar{k}_2 (\bar{e}_3 - c_2 \bar{e}_2) \\
 & \quad + f(\ddot{x}_1, \ddot{x}_{1r}, \dot{x}_1, \dot{x}_{1r}, \dot{x}_1, \dot{x}_{1r}) + \kappa_0 Q_L + \kappa_1 \hat{\Upsilon}_1 \\
 & \quad + \kappa_2 \hat{\Upsilon}_2 + \kappa_3 \hat{\Upsilon}_3] \\
 & \quad + \frac{1}{\varepsilon_1} \tilde{\Upsilon}_1 (\dot{\hat{\Upsilon}}_1 - \varepsilon_1 \sigma \kappa_1) + \frac{1}{\varepsilon_2} \tilde{\Upsilon}_2 (\dot{\hat{\Upsilon}}_2 - \varepsilon_2 \sigma \kappa_2) \\
 & \quad + \frac{1}{\varepsilon_3} \tilde{\Upsilon}_3 (\dot{\hat{\Upsilon}}_3 - \varepsilon_3 \sigma \kappa_3) \quad (54)
 \end{aligned}$$

Referring to (54), the following results can be concluded

$$\begin{aligned}
 Q_L &= (-\bar{k}_1 (\bar{e}_2 - c_1 \bar{e}_1) - \bar{k}_2 (\bar{e}_3 - c_2 \bar{e}_2) - h(\sigma + \beta \text{sgn}(\sigma)) \\
 & \quad - f(\ddot{x}_1, \ddot{x}_{1r}, \dot{x}_1, \dot{x}_{1r}, \dot{x}_1, \dot{x}_{1r}) \\
 & \quad - \hat{\Upsilon}_1 - \hat{\Upsilon}_2 - \hat{\Upsilon}_3) / \kappa_0 \quad (55)
 \end{aligned}$$

The adaptive laws are expressed as

$$\dot{\hat{\Upsilon}}_1 = \varepsilon_1 \sigma \kappa_1 \quad (56)$$

$$\dot{\hat{\Upsilon}}_2 = \varepsilon_2 \sigma \kappa_2 \quad (57)$$

$$\dot{\hat{\Upsilon}}_3 = \varepsilon_3 \sigma \kappa_3 \quad (58)$$

Substituting (55) to (58) into (54) yields that

$$\begin{aligned}
 \dot{\bar{V}}_4 &= -h\bar{k}_1^2 \bar{e}_1^2 - 2h\bar{k}_1 \bar{k}_2 \bar{e}_1 \bar{e}_2 - 2h\bar{k}_1 \bar{e}_1 \bar{e}_3 \\
 & \quad - 2h\bar{k}_2 \bar{e}_2 \bar{e}_3 - h\bar{k}_2^2 \bar{e}_2^2 \\
 & \quad - h\bar{e}_3^2 + c_1 \bar{e}_1^2 - \bar{e}_1 \bar{e}_2 + c_2 \bar{e}_2^2 - \bar{e}_2 \bar{e}_3 - h\beta |\sigma| \quad (59)
 \end{aligned}$$

and then referring to (50), we obtain

$$\dot{\bar{V}}_4 \leq -e^T Q e - h\beta |\sigma| \leq 0 \quad (60)$$

Therefore, the stability of system can be guaranteed when the matrix Q is positive definite.

For electro-hydraulic systems, the load flow Q_L of a servovalve is written as

$$Q_L = C_d \omega x_v \sqrt{\frac{P_s - \text{sgn}(x_v) P_L}{\rho}} \quad (61)$$

where C_d is valve flow coefficient, ω is valve area gradient, ρ is hydraulic oil density, P_s is pressure of oil supply system, x_v is valve spool displacement.

Due to the fact that response frequency of the EHFLS is significantly slower than that of the servo-valve, the valve spool displacement can be approximately expressed as:

$$x_v = k_v u_v \quad (62)$$

where u_v is the control voltage and k_v is a conversion factor.

Substituting (62) into (61) yields that

$$Q_L = C_d \omega k_v u_L \sqrt{\frac{P_s - \text{sgn}(u_L) P_L}{\rho}} \quad (63)$$

where u_L is the final computed voltage for obtaining the design Q_L in (55).

As for the adopted servo valve, the relationship between pressure drop and corresponding rated flow is expressed as:

$$Q_r = C_d \omega k_v u_{\max} \sqrt{\frac{\Delta P_r}{\rho}} \quad (64)$$

where u_{\max} is the saturated input voltage and ΔP_r is the certain valve pressure drop.

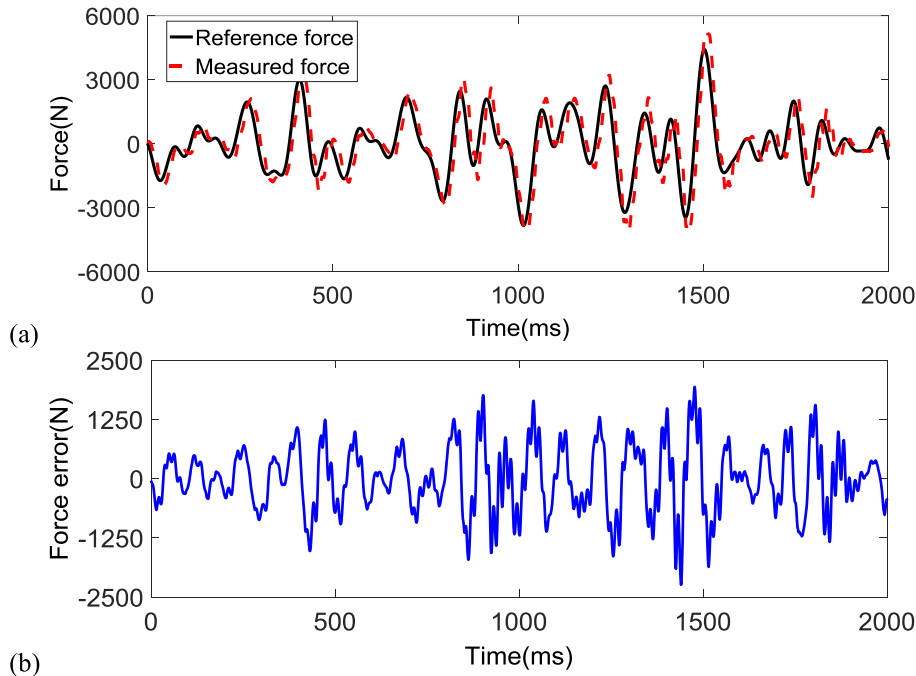


FIGURE 5. PID controller with step position external disturbances. (a) Force tracking performance. (b) Force tracking error.

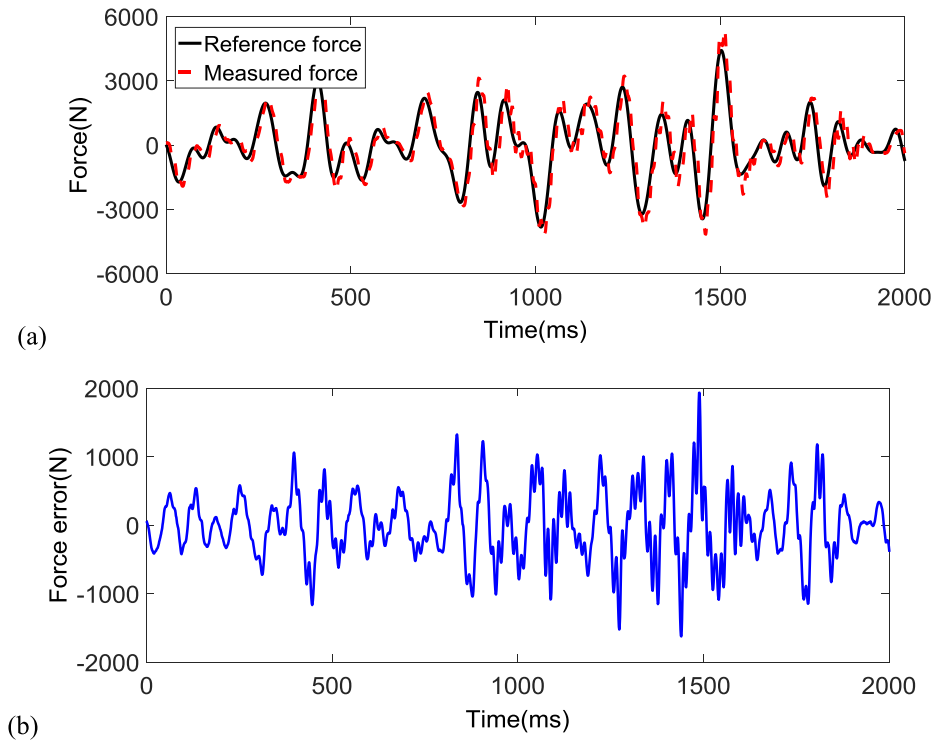


FIGURE 6. Adaptive backstepping controller (ABC) with step position external disturbances. (a) Force tracking performance. (b) Force tracking error.

Combing (63) and (64), we obtain

$$u_L = \frac{Q_L}{Q_r \sqrt{\frac{P_s - \text{sgn}(u_L)P_L}{\Delta P_r}}} u_{\max} \quad (65)$$

Owing to the fact that values of ω , C_d , k_v , and $\sqrt{\frac{P_s - \text{sgn}(u_L)P_L}{\rho}}$ are all positive, we can obtain

$$\text{sgn}(Q_L) = \text{sgn}(C_d \omega k_v u_L \sqrt{\frac{P_s - \text{sgn}(u_L)P_L}{\rho}})$$

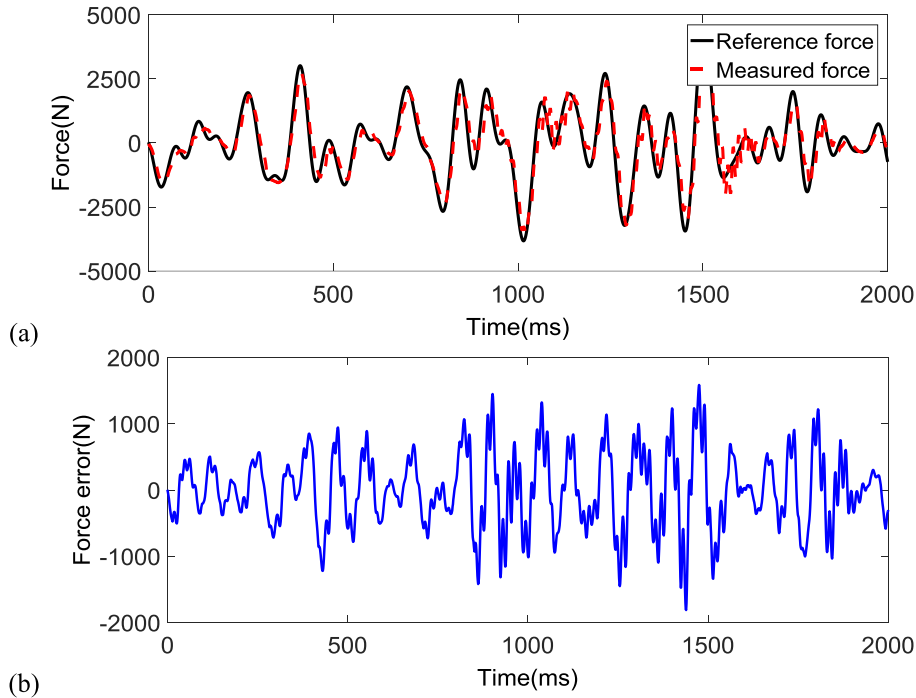


FIGURE 7. Robust adaptive sliding mode controller (RASMC) with step position external disturbances. (a) Force tracking performance. (b) Force tracking error.

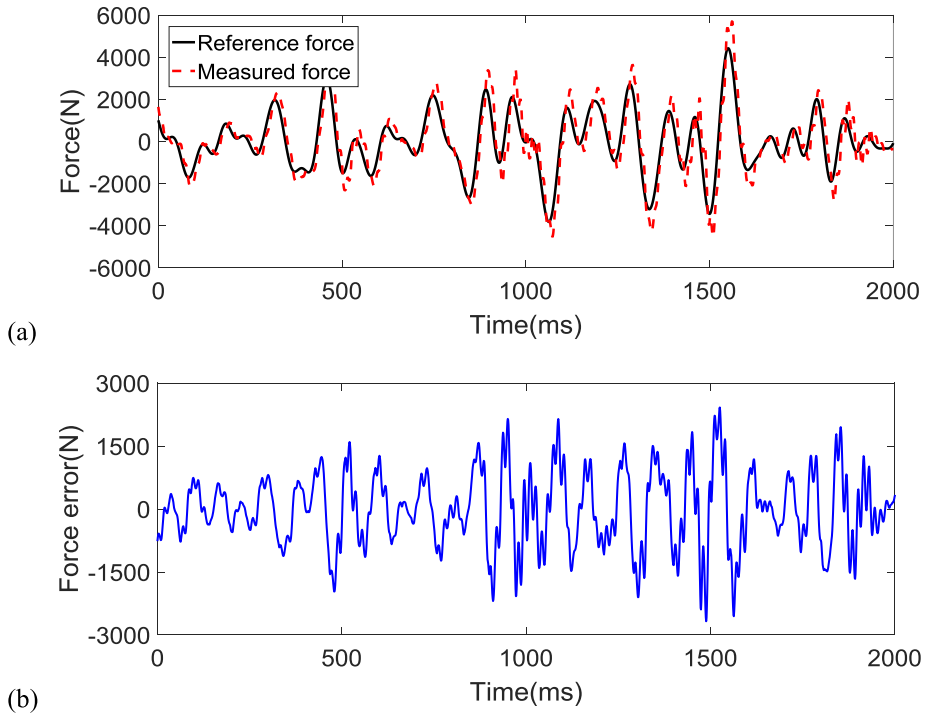


FIGURE 8. PID controller with random position external disturbances. (a) Force tracking performance. (b) Force tracking error.

$$\begin{aligned}
 &= \text{sgn}(u_L) \cdot \text{sgn}\left(C_d \omega k_v \sqrt{\frac{P_s - \text{sgn}(u_L)P_L}{\rho}}\right) \\
 &= \text{sgn}(u_L) \tag{66}
 \end{aligned}$$

and then (65) can be expressed as

$$u_L = \frac{Q_L}{Q_r \sqrt{\frac{P_s - \text{sgn}(Q_L)P_L}{\Delta P_r}}} u_{\max} \tag{67}$$

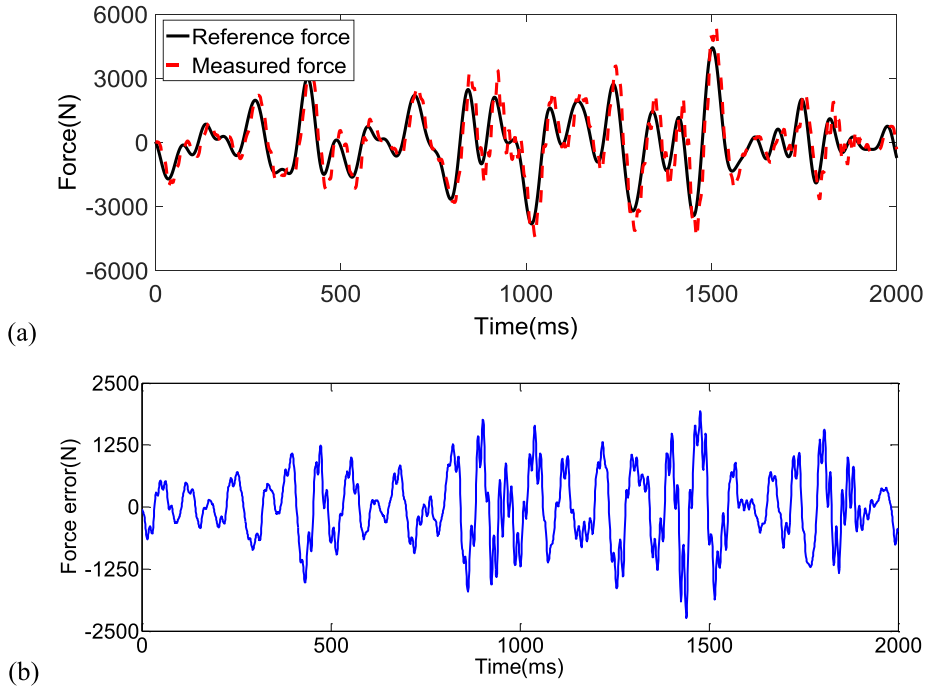


FIGURE 9. Adaptive backstepping controller (ABC) with random position external disturbances. (a) Force performance. (b) Force tracking error.

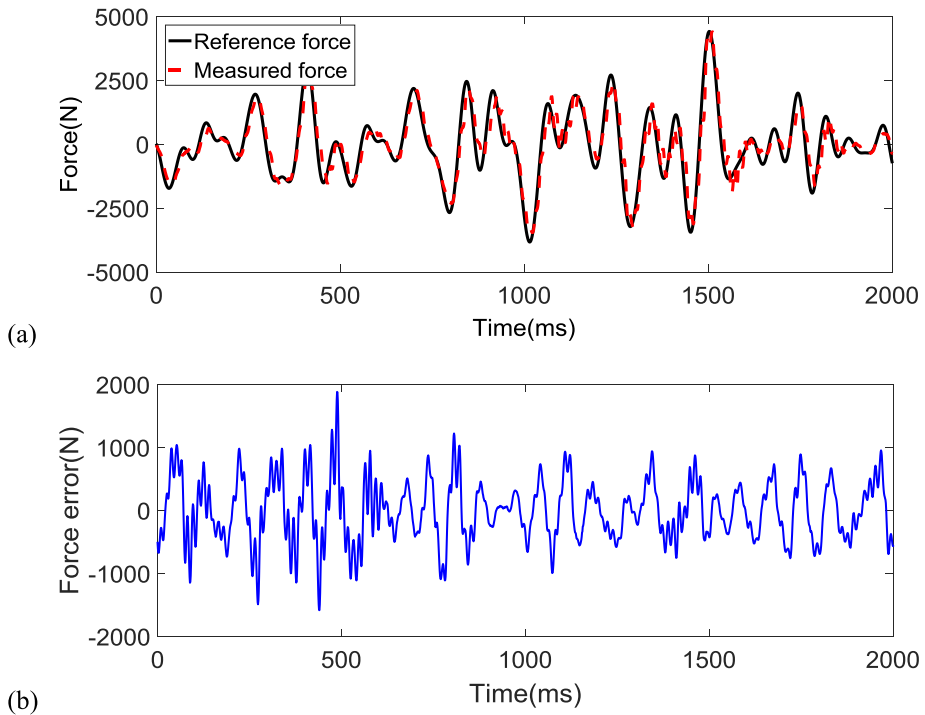


FIGURE 10. Robust adaptive sliding mode controller (RASMC) with random position external disturbances. (a) Force tracking performance. (b) Force tracking error.

IV. EXPERIMENTAL RESULTS AND ANALYSIS

In order to confirm the feasibility of the proposed controller, experiments are conducted on the established test bed, whose main parameters are shown in Table 1. In this work, the conventional PI controller, adaptive backstepping

controller (ABC), and the proposed RASMC are employed to the test bed for comparisons.

- i. PI controller: For PI controller, the control voltage is obtained just by the force tracking error, which ignores external disturbances and parameter uncertainties.

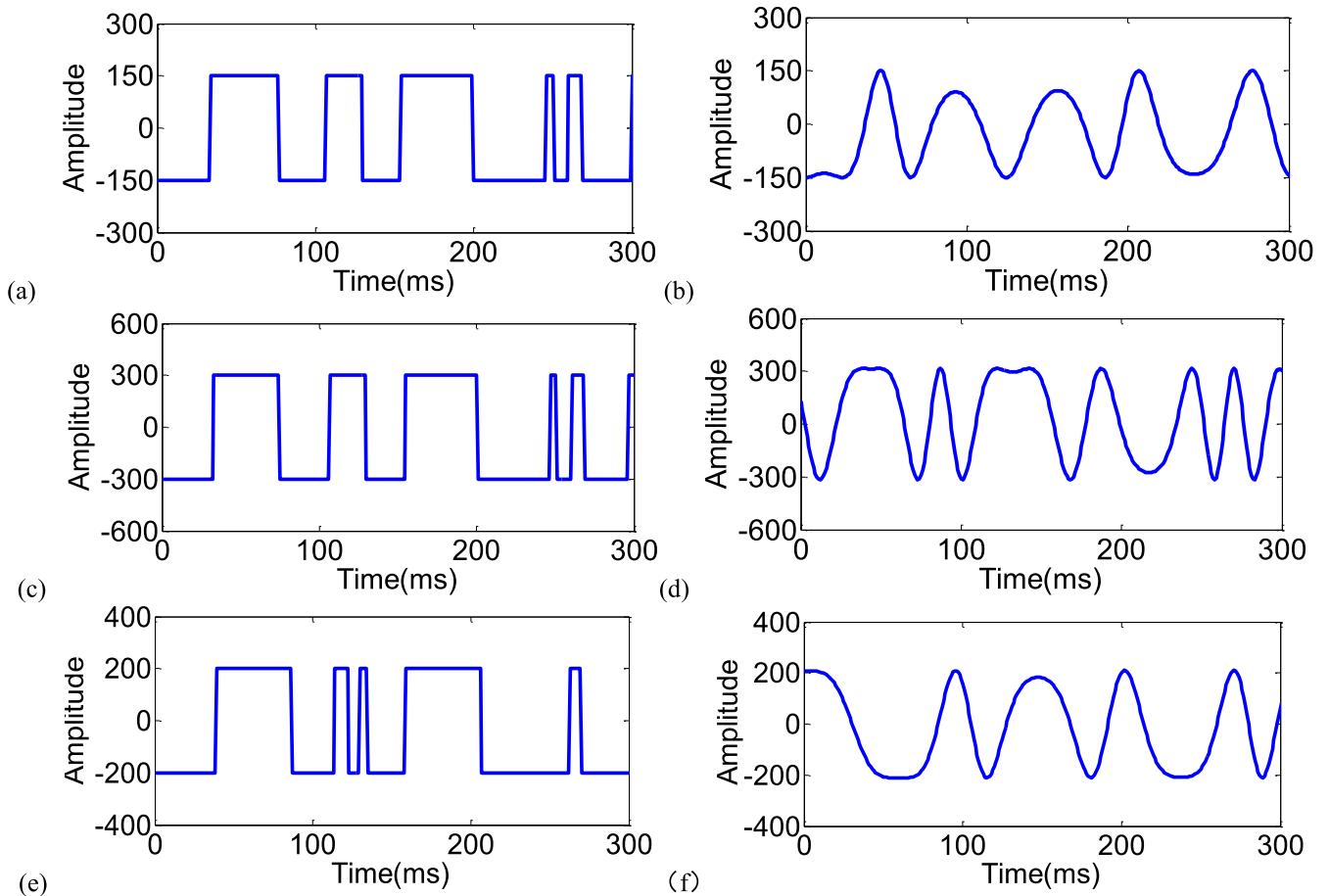


FIGURE 11. Compensation values for step position external disturbances of sign functions and sliding mode adaptive laws. (a) $F_1 \text{sgn}(e_1)$. (b) $F_2 \text{sgn}(e_2)$. (c) $F_3 \text{sgn}(e_3)$. (d) \hat{y}_1 . (e) \hat{y}_2 . (f) \hat{y}_3 .

The control voltage is computed as $u = K_p e_1 + K_I \sum e_1$, where $K_p = 0.0008$ and $K_I = 0.025$.

- ii. ABC: For the ABC, backstepping technology and adaptive updating law are employed to address parameter uncertainties and external disturbance. The control voltage is computed by (25), in which k_1 , k_2 and k_3 are gains that are employed to ensure stability of the EHFLS, whose values are $k_1 = 150$, $k_2 = 2.5 \times 10^8$, and $k_3 = 2.5 \times 10^5$. The parameter update gains are $\gamma_2 = 2.5 \times 10^{-11}$, $\gamma_4 = 4 \times 10^4$, and $\gamma_5 = 5 \times 10^{-12}$. The parameters that utilized for sign function to compensate external disturbance are $F_1 = 150$, $F_2 = 350$, and $F_3 = 200$.
- iii. RASMC: For the RASMC, sliding mode technology and adaptive updating law are employed to address parameter uncertainties and external disturbance. The control voltage is computed by (46), where h , β , c_1 , c_2 , \bar{k}_1 , and \bar{k}_2 are gains employed for stability insurance of the EHFLS, whose values are $h = 450$, $\beta = 500$, $c_1 = 8000$, $c_2 = 10000$, $\bar{k}_1 = 1000$, and $\bar{k}_2 = 1500$. The parameter update gains for the combined disturbances are $\varepsilon_1 = 500$, $\varepsilon_2 = 300$, and $\varepsilon_3 = 700$.

TABLE 1. Hydraulic parameters for EHFLS.

Description	Parameter	Value	Units
Oil effective bulk modulus	β_e	1×10^9	N/m ²
Total chamber volume	V_t	3.8×10^{-4}	m ³
Cylinder effective area	A_p	1.88×10^{-3}	m ²
Total mass	m_p	530	kg
Viscous damping coefficient	B_p	7000	N/ms ⁻¹
Stiffness of force sensor	k_f	1.9×10^7	N/m
Saturated input of servo-valve	u_{\max}	10	V
Rated flow of servo-valve	Q_r	38	L/min
Total leakage coefficient	C_{qp}	6.9×10^{-13}	m ³ /s · Pa
System supply pressure	P_s	9	Mpa

In order to compare the control performance of the adopted three different controllers, two same external disturbances including random position and step position disturbance are selected in the experiment. The random position disturbance is set as amplitude 1mm and frequency 10 Hz. The step position disturbance is set as amplitude 0.5 mm and

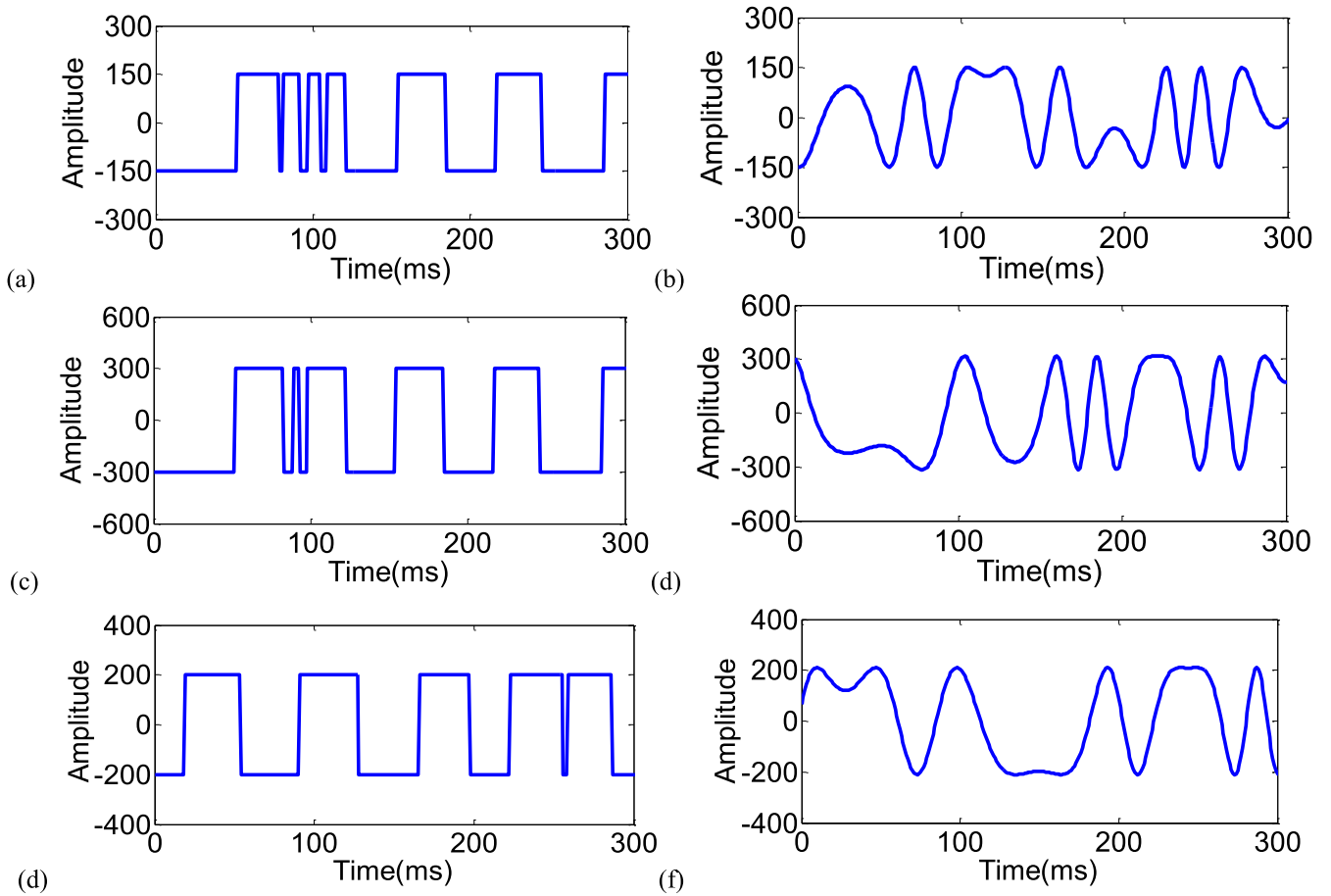


FIGURE 12. Compensation values for random position external disturbances of sign functions and sliding mode adaptive laws. (a) $F_1\text{sgn}(e_1)$. (b) $F_2\text{sgn}(e_2)$. (c) $F_3\text{sgn}(e_3)$. (d) \hat{y}_1 . (e) \hat{y}_2 . (f) \hat{y}_3 .

frequency 2 Hz. The reference force signal was set as random force, whose amplitude was set as 0.5 mm, frequency range is set as 2 Hz.

The force tracking curves and its corresponding tracking errors for the adopted three different control algorithms subjected to random position and step position external disturbance are shown in Figures 5-10, from which it can be observed that the force tracking error with the conventional PI is much bigger than that with the ABC and the proposed RASMC. As can be noticed from Figures 7-10, with the consideration of system's parameter uncertainties and external disturbance, the proposed RASMC can further alleviate the force tracking performance on chattering phenomenon resulted from the extreme external disturbances. Figure 11-12 present the compensation values for sign functions and sliding mode adaptive laws with different external disturbances. It can be noticed from Figure 11-12 that the sliding mode adaptive laws can modify the compensation values from square signal with time-varying frequency to gradually changed values.

To more effectively compare the performance of difference controllers, the root mean square error (RMSE) is utilized and

TABLE 2. Peak error and RMSE of different controller with step position external disturbances.

Control algorithm	Peak error (N)	RMSE
PID	2372.5	852.83
ABC	1934.6	637.60
RASMC	1623.5	468.53

TABLE 3. Peak error and RMSE of four control algorithms with step position external disturbances.

Control algorithm	Peak error (N)	RMSE
PID	2452.6	956.67
ABC	2031.6	757.62
RASMC	1816.5	508.93

the RMSE index is expressed as

$$RMSE(R_{in,i}, R_{out,i}, n) = \sqrt{\sum_{i=1}^n (R_{in,i} - R_{out,i})^2 / n} \quad (68)$$

where $R_{in,i}$ represents the reference signal sequence, $R_{out,i}$ represents the output signal sequence, n represents the signal length. Utilizing (68), the RMSE and peak error for force

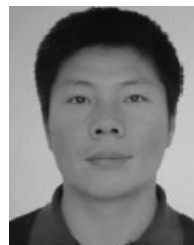
tracking performance of different controllers are exhibited in Table 2 and Table 3.

V. CONCLUSION

This article focuses on a novel robust adaptive sliding mode control method for force tracking control of EHFLS with consideration of parameter uncertainties and external disturbances. In order to obtain the proposed controller, the nonlinear model of the EHFLS is firstly established, and the system's uncertain parameters and external disturbances are merged. Then, a robust adaptive sliding mode controller is proposed, and the desired control output for the force control system in presence of parameter uncertainties and external disturbances can be obtained to guarantee the force tracking control performance. Stability of the closed-loop system with the proposed controller is analyzed using Lyapunov stability theory. The proposed controller can modify traditional adaptive backstepping controllers by suppressing chattering phenomenon resulted from the design of sign function. Experimental studies were conducted on an electro-hydraulic test bed with the help of xPC rapid prototyping technology. Experimental results indicate that the proposed controller exhibits more excellent performance on force tracking control than the conventional proportional-integral controller and adaptive backstepping controller.

REFERENCES

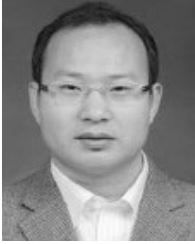
- [1] N. Nakata, "Effective force testing using a robust loop shaping controller," *Earthq. Eng. Struct. Dyn.*, vol. 42, no. 2, pp. 261–275, Feb. 2013.
- [2] A. R. Plummer, "Robust electrohydraulic force control," *Proc. Inst. Mech. Eng. I, J. Syst. Control Eng.*, vol. 221, no. 4, pp. 717–731, Jun. 2007.
- [3] H. Aknouche, H. Bechtoula, A. Airouche, and D. Benouar, "Investigation on the performance of the six DOF C.G.S., Algeria, shaking table," *Earthq. Struct.*, vol. 6, no. 5, pp. 539–560, May 2014.
- [4] J.-W. Han, J.-D. Kim, and S.-Y. Song, "Fatigue strength evaluation of a bogie frame for urban maglev train with fatigue test on full-scale test rig," *Eng. Failure Anal.*, vol. 31, pp. 412–420, Jul. 2013.
- [5] C. Guan and S. Pan, "Nonlinear adaptive robust control of single-rod electro-hydraulic actuator with unknown nonlinear parameters," *IEEE Trans. Contr. Syst. Technol.*, vol. 16, no. 3, pp. 434–445, May 2008.
- [6] X. Shao and G. Enyart, "Development of a versatile hybrid testing system for seismic experimentation," *Exp. Techn.*, vol. 38, no. 6, pp. 44–60, Nov. 2014.
- [7] S. Gang, Z. Zhen-Cai, Z. Lei, T. Yu, Y. Chi-fu, Z. Jin-song, L. Guang-Da, and H. Jun-Wei, "Adaptive feed-forward compensation for hybrid control with acceleration time waveform replication on electro-hydraulic shaking table," *Control Eng. Pract.*, vol. 21, no. 8, pp. 1128–1142, Aug. 2013.
- [8] Y. Tang, Z. Zhu, and G. Shen, "Design and experimental evaluation of feedforward controller integrating filtered-x LMS algorithm with applications to electro-hydraulic force control systems," *Proc. Inst. Mech. Eng. C, J. Mech. Eng. Sci.*, vol. 230, no. 12, pp. 1951–1967, Jul. 2016.
- [9] A. Alleyne, L. Rui, and H. Wright, "On the limitations of force tracking control for hydraulic active suspensions," in *Proc. Amer. Control Conf.*, New York, NY, USA, Jun. 1998, pp. 43–47.
- [10] A. Alleyne and R. Liu, "A simplified approach to force control for electro-hydraulic systems," *Control Eng. Pract.*, vol. 8, no. 12, pp. 1347–1356, Dec. 2000.
- [11] D. Q. Truong and K. K. Ahn, "Force control for hydraulic load simulator using self-tuning grey predictor—Fuzzy PID," *Mechatronics*, vol. 19, no. 2, pp. 233–246, Mar. 2009.
- [12] J. W. Kim, D. J. Xuan, and Y. B. Kim, "Design of a forced control system for a dynamic road simulator using QFT," *Int. J. Automot. Technol.*, vol. 9, no. 1, pp. 37–43, Feb. 2008.
- [13] J. Zhao, G. Shen, C. Yang, G. Liu, L. Yin, and J. Han, "Feel force control incorporating velocity feedforward and inverse model observer for control loading system of flight simulator," *Proc. Inst. Mech. Eng. I, J. Syst. Control Eng.*, vol. 227, no. 2, pp. 161–175, Feb. 2013.
- [14] J. Zhao, G. Shen, W. Zhu, C. Yang, and S. K. Agrawal, "Force tracking control of an electro-hydraulic control loading system on a flight simulator using inverse model control and a damping compensator," *Trans. Inst. Meas. Control*, vol. 40, no. 1, pp. 135–147, Jan. 2018.
- [15] H. Li and Y. Hu, "Robust sliding-mode backstepping design for synchronization control of cross-strict feedback hyperchaotic systems with unmatched uncertainties," *Commun. Nonlinear Sci. Numer. Simul.*, vol. 16, no. 10, pp. 3904–3913, Oct. 2011.
- [16] J. H. Park, "Synchronization of Genesio chaotic system via backstepping approach," *Chaos, Solitons Fractals*, vol. 27, no. 5, pp. 1369–1375, Mar. 2006.
- [17] C. Guan and S. Pan, "Adaptive sliding mode control of electro-hydraulic system with nonlinear unknown parameters," *Control Eng. Pract.*, vol. 16, no. 11, pp. 1275–1284, Nov. 2008.
- [18] J. Yao, Z. Jiao, and D. Ma, "High dynamic adaptive robust control of load emulator with output feedback signal," *J. Franklin Inst.*, vol. 351, no. 8, pp. 4415–4433, Aug. 2014.
- [19] C. Wang, Z. Jiao, S. Wu, and Y. Shang, "Nonlinear adaptive torque control of electro-hydraulic load system with external active motion disturbance," *Mechatronics*, vol. 24, no. 1, pp. 32–40, Feb. 2014.
- [20] T. Roy, M. Mahmud, W. Shen, A. Oo, and M. Haque, "Robust nonlinear adaptive backstepping excitation controller design for rejecting external disturbances in multimachine power systems," *Int. J. Electr. Power Energy Syst.*, vol. 84, pp. 76–86, Jan. 2017.
- [21] Q. Guo, P. Sun, J.-M. Yin, T. Yu, and D. Jiang, "Parametric adaptive estimation and backstepping control of electro-hydraulic actuator with decayed memory filter," *ISA Trans.*, vol. 62, pp. 202–214, May 2016.
- [22] A. K. Ravandi, E. Khanmirza, and K. Daneshjou, "Hybrid force/position control of robotic arms manipulating in uncertain environments based on adaptive fuzzy sliding mode control," *Appl. Soft Comput.*, vol. 70, pp. 864–874, Sep. 2018.
- [23] A. Ayadi, M. Smaoui, S. Aloui, S. Hajji, and M. Farza, "Adaptive sliding mode control with moving surface: Experimental validation for electropneumatic system," *Mech. Syst. Signal Process.*, vol. 109, pp. 27–44, Sep. 2018.
- [24] F. Plestan, Y. Shtessel, V. Brégeault, and A. Poznyak, "Sliding mode control with gain adaptation—Application to an electropneumatic actuator," *Control Eng. Pract.*, vol. 21, no. 5, pp. 679–688, May 2013.
- [25] M. Farooq, D. B. Wang, and N. Dar, "Adaptive sliding-mode hybrid force/position controller for flexible joint robot," in *Proc. IEEE Int. Conf. Mechatronics Autom.*, Aug. 2008, pp. 724–731.



LEI CHENG received the B.S. and M.S. degrees from Xi'an Jiaotong University and Jilin University, in 1990 and 1993, respectively. He is currently pursuing the Ph.D. degree with the China University of Mining and Technology. He is also the Vice-General Manager of Xuzhou XCMG Environment Technology Company, Ltd. His research interests include electrohydraulic servo control and force control.



ZHEN-CAI ZHU received the B.S., M.S., and Ph.D. degrees from the China University of Mining and Technology, in 1989, 1994, and 2000, respectively. He is currently a Professor with the School of Mechanical and Electrical Engineering, China University of Mining and Technology. He is also the Executive Vice-Dean of the Research Academy, China University of Mining and Technology. His research interests include mechanical system control and impact dynamics.



GANG SHEN received the B.S. degree from Jiamusi University, in 2005, and the M.S. and Ph.D. degrees from the Harbin Institute of Technology, in 2007 and 2011, respectively. He is currently a Professor with the School of Mechanical and Electrical Engineering, China University of Mining and Technology. His research interests include electro-hydraulic servo control, parallel robot, and loading systems.



XIANG LI received the B.S. and Ph.D. degrees from the China University of Mining and Technology, in 2013 and 2018, respectively. He holds a postdoctoral position at the School of Mechanical and Electrical Engineering, China University of Mining and Technology. His research interests include electro-hydraulic servo control, force control, and wire rope tension control of hoisting systems.



SHUJING WANG received the B.S. degree from the China University of Geosciences, in 2007. She is currently a Lecturer with Army Engineering University training base. Her research interests include mechanical engineering and hydraulic technology.



YU TANG received the B.S. and Ph.D. degrees from the China University of Mining and Technology, in 2011 and 2016, respectively. He is currently a Lecturer with the School of Mechanical and Electrical Engineering, China University of Mining and Technology. His research interests include electro-hydraulic servo control, acceleration control, and force control.

...